ANNUAL REVIEWS

Annual Review of Cell and Developmental Biology

Expansion Microscopy: Scalable and Convenient Super-Resolution Microscopy

Paul W. Tillberg[1] and Fei Chen[2]

[1]Janelia Research Campus, HHMI, Ashburn, Virginia 20147, USA; email: tillbergp@janelia.hhmi.org

[2]Broad Institute of Harvard and MIT, Boston, Massachusetts 02142, USA; email: chenf@broadinstitute.org

Annu. Rev. Cell Dev. Biol. 2019. 35:683–701

First published as a Review in Advance on August 19, 2019

The *Annual Review of Cell and Developmental Biology* is online at cellbio.annualreviews.org

https://doi.org/10.1146/annurev-cellbio-100818-125320

Keywords

super-resolution imaging, gel embedding, tissue expansion, expansion microscopy

Abstract

Expansion microscopy (ExM) is a physical form of magnification that increases the effective resolving power of any microscope. Here, we describe the fundamental principles of ExM, as well as how recently developed ExM variants build upon and apply those principles. We examine applications of ExM in cell and developmental biology for the study of nanoscale structures as well as ExM's potential for scalable mapping of nanoscale structures across large sample volumes. Finally, we explore how the unique anchoring and hydrogel embedding properties enable postexpansion molecular interrogation in a purified chemical environment. ExM promises to play an important role complementary to emerging live-cell imaging techniques, because of its relative ease of adoption and modification and its compatibility with tissue specimens up to at least 200 μm thick.

Contents

1. INTRODUCTION

Fluorescence microscopy is a fundamental tool for biologists, but the diffraction limit of light prevents interrogation with traditional fluorescence microscopy of cellular structures smaller than 250 nm. Structures in biology beyond the diffraction limit of light are ubiquitous, with almost all subcellular compartments beyond the diffraction limit. In just one example, the brain, subcellular compartments of neurons such as presynaptic terminals, postsynaptic spines, and intracellular organelles have highly intricate distributions of biomolecules. In presynaptic terminals alone, hundreds of proteins—ranging from scaffolding proteins, to proteins involved with fusing synaptic vesicles to the membrane, to mediators of synaptic plasticity—are localized for functional transmission of neuronal signaling (Shapira et al. 2003, Südhof 2004). Finally, at the tissue level, millions of neurons are arranged with synaptic connectivity patterned at the nanoscale.

In the past decade, several new technologies have emerged to allow for optical microscopy below the diffraction limit. These approaches potentially allow for ultrastructural examination of cells and tissues, a realm previously limited to electron microscopy, with light microscopy. Among the many advantages of light microscopy over electron microscopy are ease of sample preparation, ease of protein labeling, simultaneous multicolor imaging, and compatibility with in vivo imaging.

These conventional super-resolution microscopy techniques broadly fall into two main classes of improvements to optical hardware and readout modalities. First, single-molecule localization microscopy techniques [for example, stochastic optical reconstruction microscopy (STORM) and photo-activated localization microscopy (PALM)] utilize strategies to image sparse subsets of fluorophores to collect and fit statistics about the localization of single fluorophores (Betzig et al. 2006, Rust et al. 2006). Second, techniques that sculpt the illumination light to obtain higher-frequency spatial information include structured illumination microscopy (SIM), stimulated emission depletion (STED), and reversible saturable optical fluorescence transitions (RESOLFT). However, conventional super-resolution microscopes are limited by high signal-to-noise ratio (SNR) requirements, specialized hardware and software, and the detrimental effects of tissue scattering on imaging quality.

In contrast, expansion microscopy (ExM) is a physical form of magnification that increases the effective resolving power of any microscope (Chen et al. 2015). In ExM, a swellable polyelectrolyte gel is synthesized throughout the sample. During gelation, specific biomolecules such as proteins and RNA can be covalently linked into the hydrogel network. After gelation, the mechanical structure of the sample is disrupted by breaking crosslinks and bonds in proteins; however, the

anchored molecules (e.g., antibody tags, RNA, fluorescent proteins) can be retained and isotropically expanded by dialysis in water.

ExM enables nanoscale-resolution imaging of fixed cells and tissues on conventional diffraction-limited microscopes. Expanded samples are transparent and index matched to water, allowing for nanoscale imaging of large tissue volumes. ExM is easy to perform, the chemistries used are highly engineerable, and expanded specimens are compatible with a wide range of microscopy modalities. Lastly, ExM homogenizes the chemical environment of anchored biomolecules to facilitate molecular interrogation after embedding.

2. DESCRIPTION OF THE TECHNIQUE

2.1. Protocol, Principles, and Initial Validation of Expansion Microscopy

Here we describe the physical principles of ExM to give the reader an appreciation for the ExM process. The fundamental principle behind ExM is polymer embedding in a hyperswellable hydrogel. Polymer embedding has long been used in biology, including for embedding specimens for preservation (paraffin), for improved optical properties [clearing (Chung et al. 2013, Germroth et al. 1995)], or for improved mechanical properties (e.g., resin embedding for ultrathin slicing).

All such materials swell to differing extents in different solvents. In ExM, we took advantage of an additional osmotic mechanism of polyelectrolyte gels that drives swelling by orders of magnitude in volume (Tanaka et al. 1980), sufficient to contribute appreciably to imaging resolution. Polymer chains have nanoscale lengths, so we reasoned that over length scales relevant to imaging (tens of nanometers) and spanning many crosslinks in the material, fluctuations in polymer chain conformation may average out to produce uniform expansion. In most instantiations of ExM, the hydrogel is an acrylamide-acrylate copolymer crosslinked with bisacrylamide; the process is robust to changes in the monomer and crosslinker percentages, with changes in the crosslinker ratio leading to an engineerable expansion factor. In ExM, the hydrogel is formed in situ within fixed cells and tissues by first diffusing in monomers and crosslinkers before initiating free-radical polymerization. Due to the small size of the monomers and crosslinkers (~100 Da), the resulting polymer network permeates the intracellular space.

The mechanical structure of biological tissue and resulting inhomogeneous elasticity of the tissue-gel hybrid impede uniform expansion, introducing deformations unacceptable in an imaging application. Isotropy can be achieved through homogenization of the tissue mechanical properties through disruption of protein networks in fixed cells and tissues. This homogenization can be performed through many mechanisms (alkaline hydrolysis, proteolysis, and heat) (Ku et al. 2016, Tillberg et al. 2016); proteinase K, a nonspecific protease, was originally used and remains the predominant method for disruption (**Figure 1**).

Disruption techniques present a challenge for preserving signals for microscopy. Fluorescently labeled antibodies (or other affinity reagents) and fluorescent protein fusions can suffer cleavage, washout, and reduced signal intensity following disruption. The first ExM publication (Chen et al. 2015) reported an anchoring strategy for fluorescent tags through DNA-conjugated antibodies. This approach enables labeling of relevant structures through indirect immunostaining with a fluorescent DNA conjugate with a 5′ acrydite modification that can be incorporated into the hydrogel during free-radical gelation. This anchoring method can be described as indirect, wherein the fluorophore is anchored and expanded, akin to an expandable 3D cast of the structure. In subsequent publications, we and others (Chozinski et al. 2016, Tillberg et al. 2016) described direct anchoring chemistries that covalently modify protein side chains with acryloyl moieties that are incorporated during gelation (**Figure 1**). In magnified analysis of the proteome (MAP) (Ku et al. 2016), acryloyl moieties are added to proteins by reactions with formaldehyde and acrylamide.

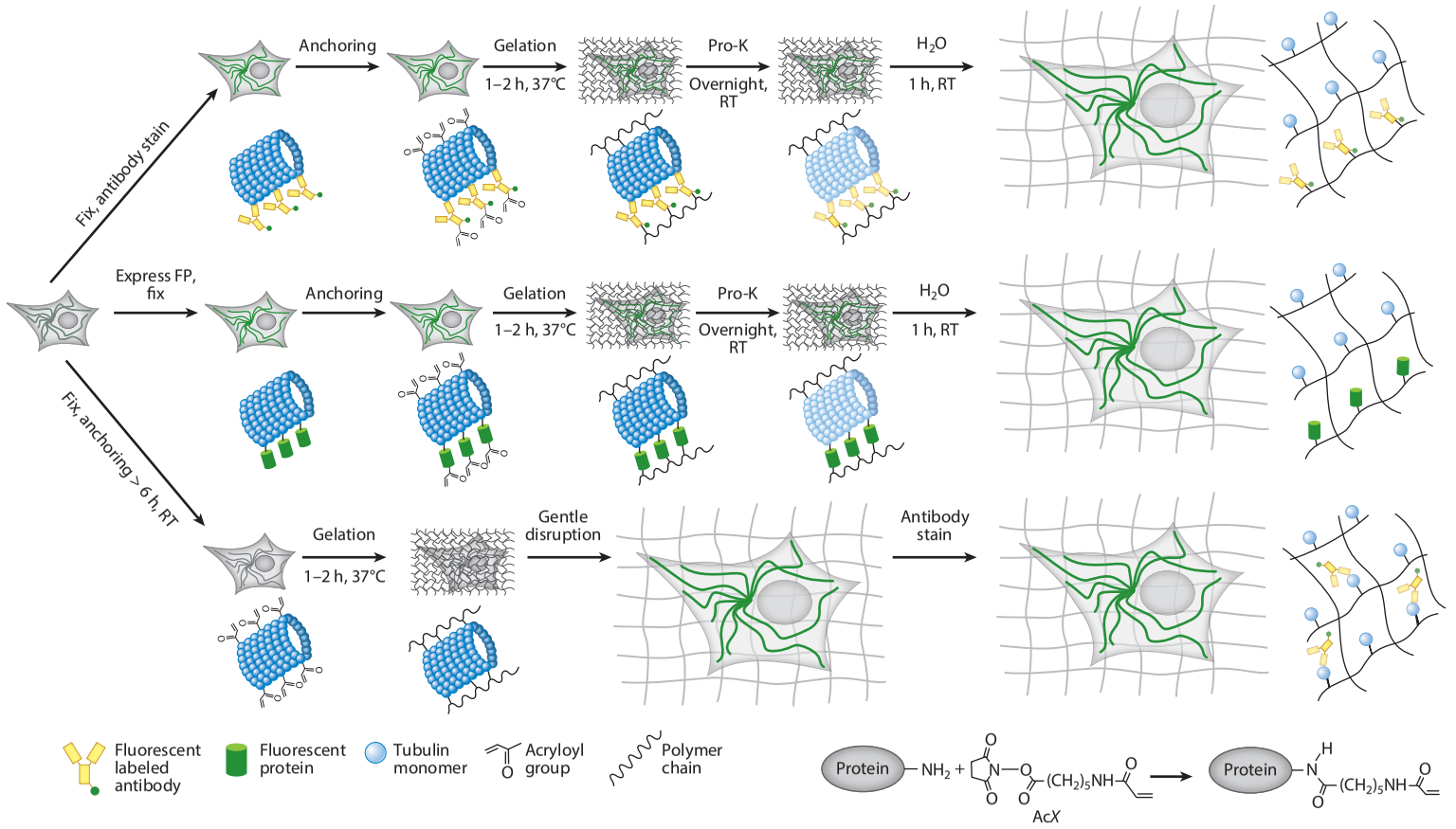

Figure 1

Schematic of the expansion microscopy (ExM) process. Shown are three different sample preparation workflows for ExM. (*Top workflow*) Samples are chemically fixed and stained with antibodies, using conventional immunostaining protocols, before anchoring treatment and subsequent ExM processing [gelation, proteinase K (Pro-K) treatment, and expansion in water]. (*Middle workflow*) Samples expressing FPs are chemically fixed and anchored before subsequent ExM processing. (*Bottom workflow*) Samples are first anchored, followed by gelation. They are then processed with a gentle homogenization procedure (for example, alkaline hydrolysis and denaturation or digestion with LysC), followed by antibody staining in the expanded state. Abbreviations, FP, fluorescent protein; RT, room temperature. Adapted with permission from Tillberg et al. (2016); copyright, Springer Nature.

These protein-anchoring approaches allow for the use of commercially available fluorescent secondary antibodies as well as direct visualization of fluorescent proteins.

We and others have extensively characterized the isotropy of expansion through this process of hydrogel embedding, anchoring, and disruption for a variety of ExM variants. The most rigorous validation involves direct comparisons between preexpansion and postexpansion imaging of the same specimen. This validation can measure expansion deformations down to the resolution of preexpansion imaging. After scaling and rigidly aligning the preexpansion and postexpansion images, a deformation vector field of the expansion process can be generated by elastically deforming the postexpansion image to align to the preexpansion image. This deformation vector field can then be used to calculate distance errors introduced by the expansion process. Using this approach and super-resolution microscopy for preexpansion imaging (SIM, STORM), we and others have found that, down to ∼50 nm, the mean error introduced by ExM is ∼1–5% of the measurement length. At the nanoscale, where direct before versus after imaging may be difficult, more indirect characterizations of ExM isotropy have been performed through measurement of structures of known dimension (see Section 3).

Thus, the broad principles of ExM can be broken down into hydrogel embedding, biomolecular anchoring, and tissue homogenization (**Figure 1**). Below, we discuss the advancement of these principles and their applications.

2.2. Expansion Microscopy Variants

Numerous groups have already begun to engineer variants of ExM. Here we describe these variants, their physical principles, and their domains of applicability. We break down these variants into three main classes: innovations in chemistry, innovations in microscopy, and applications to different specimen types.

2.2.1. Chemistry innovations. As described in Section 2.1, the polymer and anchoring chemistry are fundamental principles of ExM. As such, there are variants of ExM that modify these aspects. Several publications have modified the polymer chemistry for improved expansion factors. Chang et al. (2017) used a cleavable crosslinker to enable iterated expansion by dissolving the first gel after embedding in a second round of expandable polymerization that enabled ∼20-fold linear expansion and ∼20-nm resolution (**Figure 2*b*,*c***). In X10, a modified gelation mix, with dimethylacrylamide as a monomer in combination with sodium acrylate, was used to enable 10-fold linear expansion (Truckenbrodt et al. 2018).

In addition to improving resolution, several publications have modified the ExM chemistry steps to enable postexpansion antibody staining. These include proExM and MAP, which utilize anchoring chemistries and alternative protein disruption techniques (heat, alkaline hydrolysis, and alternative proteases) to enable postexpansion staining. UltraExM tunes fixation and anchoring conditions to enable high-density postexpansion staining of centrioles, although this was validated primarily in a cellular extract setting (Gambarotto et al. 2019).

2.2.2. Microscopy innovations. Since the expanded hydrogel is 99% water, ExM offers significant advantages for microscopy due to reduced scattering. The improved resolution and clearing are amenable to combination with recently developed light-sheet fluorescence microscopy techniques (Chen et al. 2014, Hörl et al. 2018, Huisken & Stainier 2009), with the fast volumetric throughput of light-sheet methods and effective super-resolution of ExM offering a unique solution to the resolution-throughput trade-off in microscopy (Migliori et al. 2018). Furthermore, ExM can readily be combined with existing microscopy modalities, including increasing the

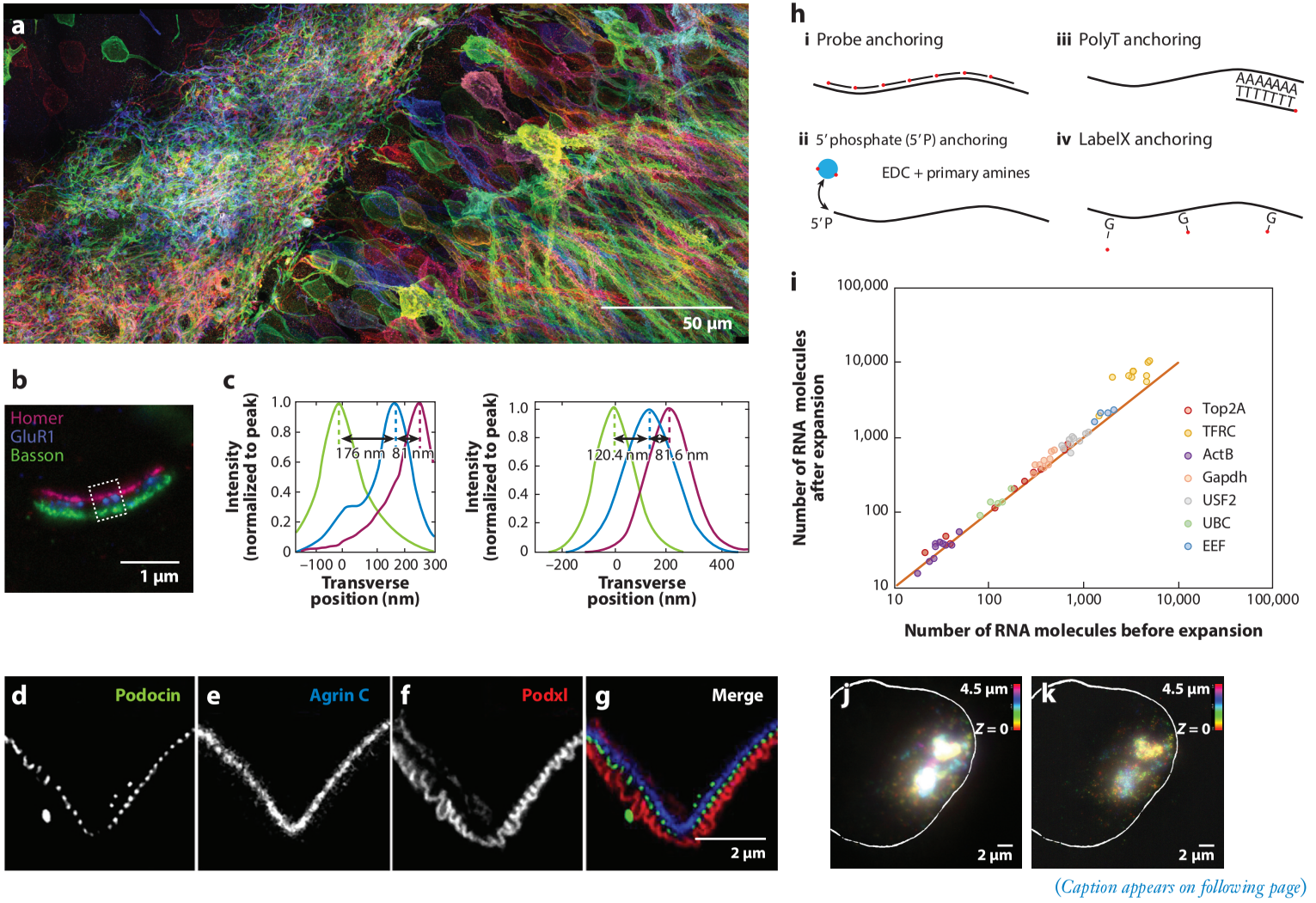

(Caption appears on following page)

Figure 2 (*Figure appears on preceding page*)

Expansion microscopy (ExM) variants. (*a*) Protein retention ExM (proExM) of fluorescent proteins and antibodies in mouse hippocampus. ProExM enables large-volume imaging of endogenous fluorescent proteins as well as conventional secondary antibodies. (*b*) Iterated expansion microscopy (iExM) of synaptic clefts. Shown is an epifluorescence image of cultured hippocampal neurons stained with antibodies against Homer1 (*magenta*), glutamate receptor 1 (GluR1, *blue*), and Bassoon (*green*), after ∼13-fold expansion via iExM. (*c*) Transverse profile of the proteins imaged in the boxed region of panel *b* (with Homer1 in *magenta*, GluR1 in *blue*, Bassoon in *green*) and sum of Gaussian functions fitted to curves for ten synapses (*thick lines*, mean; *thin lines*, ±1 SD). Notice the distinct resolution of the three protein distributions within the 200-nm synapse. (*d–g*) ExM application to nanoscale structures of mouse glomeruli. (*d–f*) Single focal plane of a glomerulus immunostained for (*d*) Podocin, (*e*) Agrin C, and (*f*) Podocalyxin (Podxl). (*g*) A merge of panels *d–f*. (*h*) Four different approaches (*i–iv*) for anchoring RNA within the hydrogel. Red circles represent gel anchorable moieties, and the wavy line denotes a nucleic acid polymer (DNA or RNA). EDC denotes 1-ethyl-3-(3-dimethylaminopropyl)carbodiimide. (*i*) Single-molecule fluorescent in situ hybridization (smFISH) characterization of anchoring yield via LabelX before versus after expansion. FISH for seven RNAs was performed over 59 cells across a 1,000-fold dynamic range (the *orange line* represents $Y = X$). (*j,k*) Representative images of expansion FISH (ExFISH). (*j*) smFISH image of XIST long noncoding RNA in the nucleus of an HEK293 cell before expansion (the *white line* denotes nuclear envelope in panels *j* and *k*). (*k*) As in panel *j*, using ExFISH. The *Z* position is color-coded. Panel *a* adapted with permission from Tillberg et al. (2016); copyright, Springer Nature. Panels *b* and *c* adapted with permission from Chang et al. (2017); copyright, Springer Nature. Panels *d–g* adapted from Chozinski et al. (2018), Creative Commons Attribution 4.0 International License. Panels *i–k* adapted with permission from Chen et al. (2016); copyright, Springer Nature.

resolution of low-cost field-deployable microscopes, as well as existing super-resolution modalities (Zhang et al. 2017). Adaptation of existing super-resolution microscopy techniques to ExM generally requires some level of modification of the ExM protocol for staining and imaging. These modifications include postexpansion sectioning of the ExM gel to reduce sample thickness for short working distance objectives (Cahoon et al. 2017, Wang et al. 2018), postexpansion gel immobilization and nanoscopic drift correction (Cang et al. 2016), and novel labeling methods that increase labeling density postexpansion (Li et al. 2018, Wang et al. 2018).

Combinations of ExM with nanoscopic methods (i.e., STED, STORM) can achieve theoretical resolutions down to 10–20 nm, but this requires validation of expansion isotropy at these length scales (see Section 3 for ultrastructural validation). An additional challenge at these resolutions are the staining densities required for Nyquist sampling; however, variants of ExM that enable postexpansion staining may reduce steric hinderance for high-density antibody labeling. Recently, modifications of fixation and gelation chemistries enabled ultraExM, which, in combination with STED, imaged purified centrioles at ∼20-nm resolution, resolving features previously seen with electron microscopy (Gambarotto et al. 2019).

2.2.3. Specimen and readout modalities. ExM has been successfully demonstrated in a variety of tissues and cells with minimal modifications. The main parameters that require tuning in a tissue type–dependent manner are the degree and type of protein disruption. For collagenous tissues and strongly fixed clinical samples, several ExM publications have modified the protease digestion to include collagenase, EDTA, and stronger protease treatments (Chozinski et al. 2018, Unnersjö-Jess et al. 2018, Zhao et al. 2017) (**Figure 2*d–g***). ExM has also been adopted to whole-mount zebrafish embryos (Freifeld et al. 2017), as well as whole *Drosophila* brains, with minimal modifications to the protease digestion.

ExM has additionally been readily applied to readout modalities beyond fluorescent imaging of proteins. We and others have demonstrated RNA anchoring (see Section 4 and **Figure 2*g–j***) to enable fluorescent in situ hybridization (FISH) imaging of RNAs in the expanded state (Chen et al. 2016). This approach has been extended to highly multiplexed detection of RNAs, including exMERFISH (Wang et al. 2018). ExM has also been used with nonfluorescent imaging modalities, including the imaging of plasmonic nanoparticles using surface-enhanced Raman scattering spectroscopy (SERS) and dark-field spectroscopy (Artur et al. 2017, 2018). Nonfluorescent approaches such as SERS may enable significant multiplexing and improved SNR and photostability

(Wei et al. 2017). Intriguingly, an expansion-based process was used with molecular crystals of ferritin in combination with X-ray diffraction (XRD) to potentially improve XRD data (Zhang et al. 2018).

3. EXPANSION MICROSCOPY TO STUDY NANOSCALE STRUCTURES

While live-cell imaging technology is advancing rapidly to provide a detailed organelle-level view of cell biology (Chen et al. 2014, Chhetri et al. 2015) and of the nanoscale dynamics of fluorescently tagged proteins (Godin et al. 2014, Liu & Tjian 2018), super-resolution microscopy in fixed and antibody-stained specimens has a complementary role to play in uncovering the protein-level structure underlying this mechanistic picture. ExM in particular is a robust method to circumvent the diffraction limit, with low setup and recurring costs, and is compatible with a wide range of upstream tissue-processing steps, making it an ideal choice for labs that are not specialized in super-resolution imaging (Zhang et al. 2017). In addition to this democratizing potential, ExM provides the same resolution enhancement in the axial dimension as in the lateral dimensions, readily allows for multicolor super-resolution, and can be done easily throughout thick tissue specimens.

Many of the initial uses of ExM to study suborganelle structure have been in neurons. One question of particular importance is how to separate pre- and postsynaptic mechanisms of signal transduction and synaptic development and plasticity (Costa et al. 2017), a task made challenging by the subdiffraction limited proximity of these compartments. Mosca et al. (2017) used a combination of ExM and more traditional knockout and overexpression methods to demonstrate a role for the protein LRP4, localized in presynaptic compartments, in directing the development of excitatory synapses. Here, expansion was used to confirm the colocalization of LRP4 with the known presynaptic protein Bruchpilot, within the context of dense neuropil. Hafner et al. (2018) used ExM to study the subsynaptic localization of protein synthesis in cultured neurons. Antibodies against vesicular neurotransmitter transporters were used to identify excitatory and inhibitory presynaptic compartments, while postsynaptic compartments were identified by the expression of the fluorescent protein mCherry. Oligonucleotide probes against the polyA tail of mRNA and 28S rRNA were used to identify the materials needed for protein synthesis, and metabolic labeling was used to identify nascent protein prior to expansion (Hafner et al. 2018).

Other subcellular compartments such as mitochondria can similarly be studied using ExM. Suofu et al. (2017) used ExM in a study of the suborganelle distribution of melatonin signaling pathways in isolated mitochondria. After expansion, the outer mitochondrial membrane (OMM) (marked by anti-TOM20) was clearly distinguishable from the matrix and contained melatonin receptor 1, which can bind to extramitochondrial melatonin (Suofu et al. 2017). Fecher et al. (2018) used ExM to confirm localization of a new construct (OMM-localized GFP, to pull down mitochondria from genetically defined cell types) on the OMM in brain tissue after confirming localization to mitochondria by using standard microscopy (Fecher et al. 2018).

The robust, inexpensive fourfold-resolution boost offered by ExM can be supplemented by combining ExM with the routine super-resolution methods SIM and Airyscan. These methods do not match the resolution of STORM, PALM, and STED, and they do require specialized equipment, but they are relatively easy to use. Cahoon et al. (2017) used ExM followed by SIM (ExSIM) in *Drosophila* to study the 3D structure of the synaptonemal complex (SC), an elaborate structure that facilitates crossing over between sister chromatids during meiosis. In this study, the SC structure known from electron microscopy was supplemented with numerous antibody stains for specific proteins, including their axial distribution. Another group used ExSIM to study the cytoskeleton of the parasite *Giardia* (Halpern et al. 2017) (**Figure 3*a***). Electron microscopy had

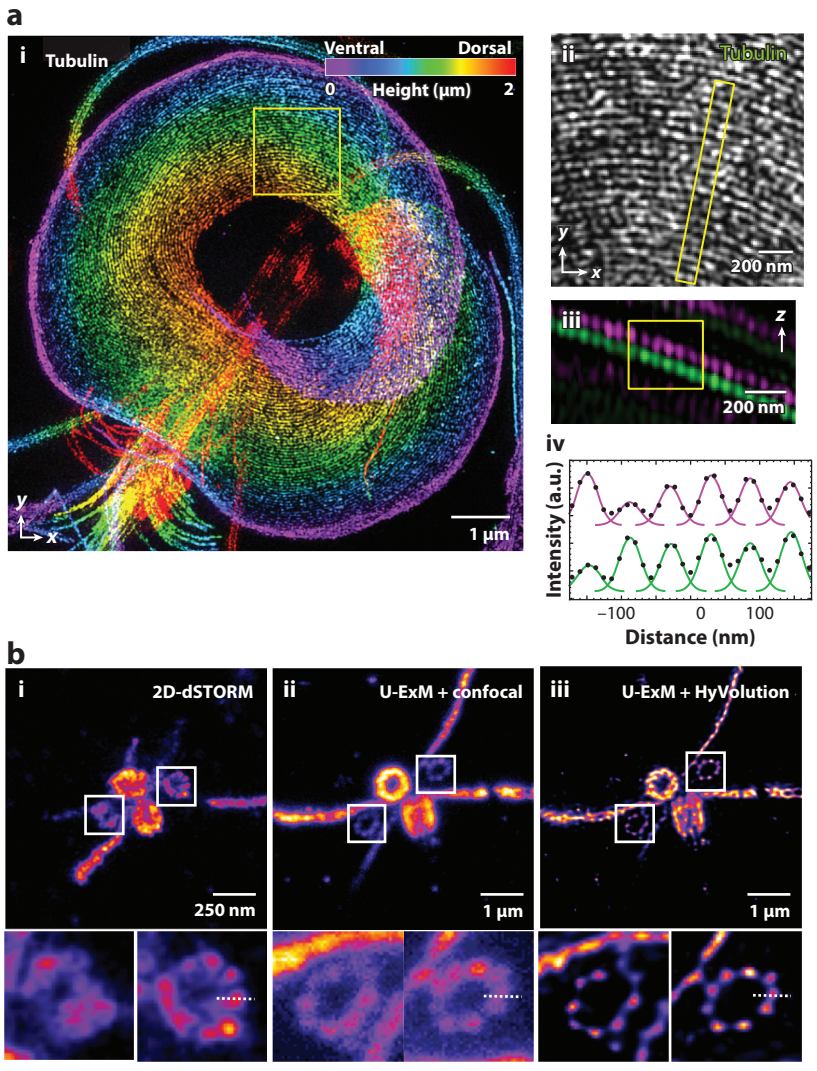

Figure 3

Expansion microscopy reveals sub-100-nm features of cytoskeletal structures. (*a*) Expanded *Giardia* cell imaged with structured illumination microscopy (SIM), focusing on the adhesive disk. (*i*) Antibody stain for tubulin showing overall cytoskeleton structure with color-coded height. (*ii*) Zoom-in of yellow boxed region in subpanel *i* showing microtubules spaced at ∼60 nm. (*iii*) Cross-section projection of the yellow boxed region in subpanel *ii* showing DAP86676 (*magenta*) lying ∼60 nm above each microtubule, coincident with the microribbon structure known from electron microscopy. (*iv*) Line profiles (*dots*) and Gaussian fits (*solid lines*) of intensity from the yellow boxed region in subpanel *iii*. Scale bars, 1 μm (*i*) and 200 nm (*ii–iv*), scaled to preexpansion sizes. Panel *a* adapted with permission from Halpern et al. (2017); copyright, ACS Publications. (*b*) Centrioles isolated from *Chlamydomonas* and antibody stained for tubulin after expansion using an ultraExM (U-ExM) procedure imaged by direct STORM (dSTORM) (*i*, *top*) and by expansion followed by confocal (*ii*, *top*) and HyVolution (*iii*, *top*) microscopy. (*i–iii*, *bottom*) Zoom-ins of white boxed regions in *i–iii*, top. Scale bars 250 nm (*i*) and 1 μm (postexpansion) (*ii*,*iii*). Panel *b* adapted with permission from Gambarotto et al. (2019); copyright, Nature Publishing Group.

previously been used to characterize the elaborate ultrastructure of the *Giardia* adhesive disk, which features microtubules spaced at 40–70 nm apart—too close to resolve using ExM or SIM alone—and associated microribbons. Halpern et al. (2017) resolved these structures by using ExSIM and annotated them with the relative positions of several proteins.

Expanded specimens can also be imaged using the Zeiss Airyscan system. Goonawardane et al. (2018) used this method to study the distribution of the protein NS5A and its phosphorylated form (pS225) in cells infected with hepatitis C. These authors had previously identified NS5A clusters with direct STORM (dSTORM) in only one color. ExM allowed them to look at both pS225 and total NS5A and to resolve the localization of pS225 within the larger NS5A clusters. By imaging these structures in 3D, they found that pS225 colocalized specifically with the edges of holes in the clusters. Tsai et al. (2017) used expansion followed by Airyscan to study the distribution of the transcription factor ultrabithorax (Ubx) in the nuclei of *Drosophila* embryos. Using Airyscan on unexpanded specimens, they saw Ubx distribution was not uniform, while expansion provided a higher-resolution view, enabling counting of the Ubx clusters (Tsai et al. 2017).

Expanded specimens can also be imaged with the higher-resolution methods. Pesce et al. (2018) imaged nuclear pore complexes (NPCs) using STED on expanded specimens to test the isotropy of ExM. Compared with the clathrin-coated pits characterized by Chen et al. (2015), nuclear pores are smaller (∼60 nm versus ∼130 nm) and more uniform, with a stereotyped eightfold-symmetric arrangement of dozens of NPC proteins. Pesce et al. (2018) carried out a careful analysis of expansion factor on several length scales: angular distribution of NPC subunits, NPC diameter, distance between NPCs within a nucleus, distance between nuclei, and the overall size of the gel. As observed by Chen et al. (2015), the gel expands by ∼5×, while the distance between nuclei expands by ∼4.3×. This consistent discrepancy may be due to shrinkage of the tissue in the high-salt ExM monomer solution. NPC expansion at 4.3× matched the internucleus expansion exactly, while the distance between NPCs expanded ∼3.8×, approximately 10% less than the internucleus expansion. The eightfold symmetry, while degraded due to imperfect antibody labeling, as with any antibody-based imaging method, was roughly preserved. Thus, the original ExM method was found to preserve the ultrastructure of NPCs to the point at which the quality of antibody stain is the primary limit on structure determination. The observed low intranuclear expansion could be a result of residual tissue integrity due to genomic DNA, which is not digested by the strong protease step, a topic that merits further study.

At the resolution levels of STED performed on expanded specimens, antibody artifacts become a limiting factor for performance (Whelan & Bell 2015). Native tissue, even after fixation and permeabilization, is a crowded, chemically complex environment, while antibodies at 120 kDa are large proteins. Steric hindrance limits the efficiency of antibody-epitope binding, while the size of the antibody (∼10 nm for each primary and secondary antibody) directly introduces a localization error. Smaller antibody fragments partially address these issues (Beghein & Gettemans 2017), but do so at the expense of reduced signal amplification (which is particularly important when one is imaging in thick tissue specimens with relatively lower numerical aperture microscope objectives) and do not take advantage of the tremendous library of traditional antibodies that is now commercially available. Carrying out antibody staining after expansion (Ku et al. 2016, Tillberg et al. 2016) may improve these currently fundamental limits. Gambarotto et al. (2019) carried out a careful optimization and analysis of postexpansion staining of centrioles by using a modified ExM gel recipe and several imaging modalities (**Figure 3*b***). Centrioles are excellent reference structures, as they have a stereotyped structure on several length scales known from electron microscopy: microtubule triplets, arranged at specified angles relative to each other and forming a bundle with known diameter. Gambarotto et al. found that all of these levels of structure were preserved and in fact showed higher fidelity to the known structure relative to dSTORM carried out on

unexpanded antibody-stained specimens, likely due to reduced competition between antibodies for closely spaced epitopes in the expanded state. The modified protocol is compatible with fixed cells in addition to isolated centrioles, but it will be important to validate that the ultrastructural preservation is equally good in this more complex context.

4. MAPPING NANOSCALE STRUCTURES OVER LARGE TISSUE VOLUMES

Beyond convenience and low cost, ExM has the added benefit of rendering the specimen nearly completely transparent and index matched to water. A fourfold linear expansion corresponds to a 64-fold volumetric expansion and concomitant dilution of any biomolecules remaining after a digestion step featuring strong detergent and a promiscuous protease. This clearing allows for ready optical access to thick tissue slices and excellent index matching for water-matched objective lenses, providing equal imaging performance throughout tissue slices whose thickness is in principle limited only by the working distance of the objective lens (divided by the expansion factor). Thus, ExM readily enables subdiffraction limited imaging over tissue slices at least hundreds of micrometers thick and with lateral sizes limited only by the geometry of the microscope stage. This multiscale imaging capability has been demonstrated in multiple tissues, including clinical human specimens (Zhao et al. 2017), mouse and human kidney (Chozinski et al. 2018), *Drosophila* embryos (Tsai et al. 2017), and zebrafish larvae (Freifeld et al. 2017). Thus, the democratizing potential of ExM for super-resolution and cell biology can be extended to researchers interested in biology at higher levels of tissue organization and to specimens of relevance to clinical diagnosis.

This capability has particular promise for studying brain tissue, where neural circuits are characterized by exquisite organization coordinated simultaneously over many length scales, from synapses patterned on the submicrometer scale, to full dendritic arbors on the hundred-micrometer scale and axon projections spanning up to the entire central nervous system. The regionalized view of the brain, in which each part of the brain is responsible for carrying out a discrete task, is now being updated with the realization that a behavior often cannot be understood without considering multiple regions simultaneously (Guo et al. 2017, Kim et al. 2016). Thus, the significance of any one synapse depends on its context within neural circuits that can span multiple regions of the brain. By giving researchers ready access to subdiffraction limited structures over macroscopic distances, ExM will have an important role to play in studying the anatomy of these distributed and micropatterned networks.

Guo et al. (2018) used ExM as part of a study of a newly discovered projection pattern connecting brain regions in *Drosophila* that had been known to regulate different aspects of sleep: (*a*) a circadian circuit that tracks time of day and (*b*) a homeostatic circuit that tracks the animal's need for sleep. A particular set of neurons from the circadian circuit [anterior-projecting dorsal neurons (APDNs)] was found to synapse onto a set of neurons [tubercular-bulbar (TuBu) neurons] that in turn project to ellipsoid body neurons, which are involved in sleep homeostasis. ExM was used to examine in detail the dense neuropil region in which the APDN axons contact TuBu dendrites (Guo et al. 2018). This study used physiological methods to confirm the synaptic connection between these neurons—doing so through microscopy requires the identification of synaptic proteins or ultrastructure. In the case of *Drosophila*, the nc82 antibody against the synaptic protein Bruchpilot is a good candidate for this role (Laissue et al. 1999). In conjunction with higher expansion levels to achieve ~50-nm resolution (Hörl et al. 2018) and resolve closely apposed neurites, this approach may allow for the unambiguous identification of synaptic connections between closely apposed neurites. In this way, entire neural circuits such as those incorporating the genetically defined fruitless set of neurons in *Drosophila* (Yu et al. 2010) may

soon be traceable in expanded brains. Compared with similar efforts to trace neural circuits in electron microscopy images, this approach of sparse tracing allows throughput to be substantially increased, potentially allowing comparisons to be made among multiple individuals in different experimental conditions or from different, closely related species.

With diffraction-limited imaging, projectomics datasets do not include direct evidence of synaptic connections and either forgo single-neuron resolution (Kuan et al. 2015) or proceed with a limited number of neurons labeled in each brain (Economo et al. 2016). ExM promises to allow neural projections to be characterized at single-neuron resolution, with significant fractions of neurons included per brain and with synaptic proteins imaged at the resolution required to identify synaptic partners. Furthermore, the robustness of ExM allows it to be combined with other data modalities, including mRNA FISH and multiplexed antibody staining, or to be conducted on tissue that has been characterized by in vivo methods. Adding molecular information is especially important in vertebrates, in which genetic tools are harder to use and circuit structure is less stereotyped than in *Drosophila*. In short, ExM will allow researchers to study not just projection and connection patterns but also their relationship with neuronal cell types and circuit function.

Just as ExM was used to annotate the ultrastructure of *Giardia* cytoskeletal microribbons with protein identifications (Halpern et al. 2017), ExM will be well suited to studying the molecular composition underlying the complex ultrastructure of synapses (Burette et al. 2012). STORM and STED are currently being deployed to study the nanoscale organization of synaptic proteins and their functional consequences (Biederer et al. 2017, Fulterer et al. 2018). ExM, particularly with higher expansion factors or in combination with SIM, will allow this variation to be observed readily over larger tissue volumes, including the entire *Drosophila* brain, and with the throughput necessary to observe variation among multiple experimental conditions.

ExM has also been used to study glia (Wang et al. 2016), which are increasingly recognized as shaping synaptic function. The complex structure of a synapse can extend beyond the synapse itself to include a surrounding glial sheath. The entire structure of pre- and postsynaptic sites and glial sheath, termed the tripartite synapse (Perea et al. 2009), has been studied using electron microscopy and is thought to play an important role in regulating the levels and time course of neurotransmitter presence in those synapses and the level of neurotransmitter spillover into the extrasynaptic space. Glomeruli, comprising multiple pre- and postsynaptic partners forming a cluster of synapses all bounded by one glial ensheathment, may carry out computational tasks beyond the actions of single synapses (Mapelli et al. 2014). ExM allows these structures to be imaged readily across extended neural circuits, with the full range of multiplexing available through commercial antibodies.

Several other multicell microstructures in brain have been studied using ExM. Deshpande et al. (2017) used ExM to assess the distribution of the gap junction protein connexin43, relative to the submicrometer-level structure of glia and endothelial cells of the blood-brain barrier, in brain tissue from human patients with temporal lobe epilepsy. Crittenden et al. (2016) discovered a novel arrangement of neurites in rodent brain, termed a bouquet, in which axons from striosomal neurons project through the substantia nigra par compacta (SNc) and form a bundle with descending dendrites from dopaminergic SNc neurons on their way to the substantia nigra pars reticulata (**Figure 4*a***). ExM was used to explore this complex 3D structure in greater detail than possible with confocal microscopy alone, clearly demonstrating the finely interdigitated arrangement of striosomal and dopaminergic neurons within the bouquet. In a tour de force demonstration, Gao et al. (2019) used ExM combined with lattice light-sheet imaging to characterize the morphology of neuronal mitochondria, lysosomes, synapses, and dendritic spines in mouse brain (**Figure 4*b***). They also imaged entire expanded *Drosophila* brains, tracing bundles of

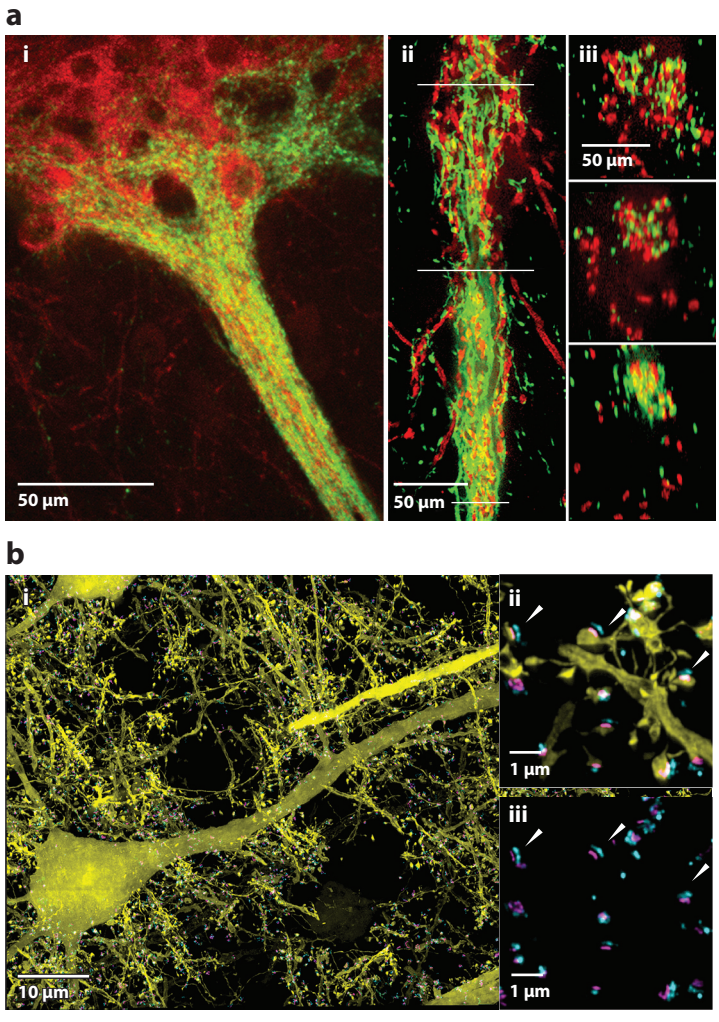

Figure 4

Expansion microscopy for extended tissue volumes. (*a*) A striosome-dendron bouquet with ventrally extending dendrites of substantia nigra pars compacta dopaminergic neurons (*red*) tightly bundled with striosomal axons (*green*). (*i*,*ii*) The bouquet imaged with confocal microscopy (*i*) before and (*ii*) after expansion. The horizontal lines in subpanel *ii* indicate positions of the cross sections shown in subpanel *iii*. (*iii*) Cross sections from subpanel *ii*, illustrating axial resolution and clearly resolving striosomal and dopaminergic fibers. Scale bars, 50 µm (*i*) and 50 µm (postexpansion) (*ii*,*iii*). Adapted with permission from Crittenden et al. (2016). (*b*) Lattice light-sheet imaging (maximum intensity projection of a 9.3-µm slab) of expanded mouse brain. (*i*) Yellow fluorescent protein (YFP)-expressing pyramidal neurons (*yellow*). (*ii*,*iii*) Zoom-in of synapses stained for presynaptic Bassoon (*cyan*) and postsynaptic Homer1 (*magenta*), indicated by arrowheads, showing colocalization of postsynaptic Homer1 with dendritic spines (*ii*) expressing YFP and (*iii*) without the YFP channel, showing clear separation between the pre- and postsynaptic stains. Scale bars, 10 µm (*i*) and 1 µm (*ii*,*iii*), scaled to preexpansion sizes. Adapted with permission from Gao et al. (2019); copyright, AAAS.

axons from olfactory projection neurons and automatically identifying synapses throughout the brain by segmenting anti-Bruchpilot antibody stain puncta (Gao et al. 2019).

5. ENGINEERED HYDROGEL ENVIRONMENTS FOR POSTEXPANSION MOLECULAR INTERROGATION

Following strong protease digestion and gel expansion, biomolecules from the tissue have been removed from the chemically complex environment of their native tissue to the engineered environment of the gel material. The digestion process, carried out on gel-anchored tissue, can be thought of as an antigen retrieval method pushed to an extreme limit with no need to balance the strength of the process and maintaining the structural integrity of the tissue. This transformation may facilitate downstream operations on the tissue, such as antibody staining, amplification, or enzymatic processes. The transformation of the tissue environment is accompanied by strong decrowding of the native biomolecules, which is particularly useful for highly multiplexed or single-molecule studies of mRNA.

Fundamental to this process is chemistry to anchor biomolecules to the hydrogel in situ. Anchoring of biomolecules in hydrogels has many advantages in addition to the increase in resolution through ExM. The ability to surround biomolecules such as RNA with pure, user-specified chemical environments vastly opens up analytical possibilities, converting the difficult in situ environment into a more reliable classical biochemical environment that allows for facile reagent exchanges and physical space for signal amplification. Anchoring chemistry has been developed to anchor tags, proteins, and nucleic acids such as RNA.

Protein anchoring approaches broadly take advantage of covalent linkages of the polymer network to protein side chains. In proExM and MAP, *N*-hydroxyl-succimidyl ester chemistry (acryloyl-X and *N*-hydroxysuccinimide acrylate) are used to modify primary amines on proteins with aryloyl side chains prior to gelation. In MAP, covalent attachment of acrylamide to proteins is accomplished through formaldehyde crosslinking to nucleophilic side chains (Ku et al. 2016). Protein anchoring enables antibody staining in the expanded state, which can relieve steric hindrance on antibody stain density (Gambarotto et al. 2019). ExM essentially uncouples the trade-off between tissue preservation and epitope recovery that is inherent in antigen retrieval.

Current anchoring approaches for nucleic acids can be broken down into two broad categories: hybridization-based approaches and chemical anchoring approaches. In hybridization-based approaches, oligonucleotide probes that are complementary to specific RNAs or generally bind classes of RNAs are modified with an acryloyl moiety (e.g., 5′ acrydite) to enable incorporation during free-radical polymerization (Kenney et al. 1998, Tsanov et al. 2016). Hybridization-based anchoring offers several advantages: First, it requires no chemical modification of nucleic acids, and second, probe design for targeted anchoring is identical to FISH, and oligo-dT anchoring requires only one oligo sequence. However, these approaches are limited by generalizability, and the targeted approach does not readily scale to many RNAs, while oligo-dT anchoring is limited to polyadenylated RNAs.

In chemical anchoring approaches, nucleic acids (i.e., DNA, RNA) are modified with acryloyl moieties directly in situ before incorporation via free-radical-mediated polymerization into the polymer backbone (**Figure 2*f***). Two chemical anchoring strategies have been demonstrated in the literature: (*a*) 5′ phosphate end labeling with carbodiimide and (*b*) direct base alkylation. In the carbodiimide crosslinking strategy, RNA is anchored after gelation via 1-ethyl-3-(3-dimethylaminopropyl)carbodiimide reactions to the 5′ terminal phosphate of RNA to amines on proteins or the acrylamide side chains (Hermanson 2013, Pena et al. 2009, Sylwestrak et al. 2016). This strategy is potentially generalizable to all nucleic acids but has downsides. First, not all RNAs

have 5′ terminal phosphates available for reaction, such as 5′ capped RNA. Second, the reaction preferentially reacts to primary amines on proteins and is thus not robust to protein digestion during expansion. In ExFISH, an anchoring molecule was synthesized; this molecule contains both an alkylating group that reacts primarily to the N7 of guanine and a polymerizable acrylamide moiety from commercially available reagents (Chen et al. 2016). This strategy is generalizable and scalable to all nucleic acids, allowing for highly efficient covalent linkage of mRNAs to the hydrogel matrix. This direct covalent linkage allows for protein digestion during expansion, as well as washout of nonanchored components.

Anchoring of nucleic acid components enables postexpansion in situ hybridization of RNA (FISH). Expansion mediates decrowding of RNA to resolve densely packed transcripts in noncoding RNAs such as *XIST* and *NEAT1*, as well as highly multiplexed FISH (Chen et al. 2016). More fundamentally, temporal barcoding through iterative imaging of transcripts requires that individual RNAs be spatially resolved, which rapidly becomes challenging for imaging large panels of many RNAs without the high resolution afforded by ExM. Thus, RNA density is often limiting when many highly expressed genes are targeted; in Wang et al. (2018), expansion enabled an order-of-magnitude increase in profiled RNA density with MERFISH.

Finally, anchoring converts the tissue into a user-controlled chemical environment. By removing proteins and lipids, the anchored molecules are effectively purified from the tissue in the hydrogel. This aspect may offer an engineerable environment to perform enzymatic processes in situ. Recently, several groups have developed approaches for in situ RNA amplification and sequencing. These approaches rely on enzymatic amplification through reverse transcription, ligation, and rolling circle amplification to generate in situ sequencing libraries (Ke et al. 2013, Lee et al. 2014). These enzymatic reactions may be improved when RNAs are purified of contaminating proteins and through the molecular decrowding process of expansion. Thus, expansion may, in the future, be an ideal platform for in situ molecular interrogations of nucleic acids via sequencing.

6. CONCLUSION

ExM is a low-cost, simple method to circumvent the diffraction limit of optical microscopy without specialized equipment or image processing. The method is robust and compatible with a wide range of tissue preparation procedures, including the use of thick (up to at least 200 μm) tissue slices. The primary insight driving ExM is that tissue can be embedded into a hyperswellable material and dissolved down to molecular-scale fragments, and the isolated fragments can then be isotropically expanded by the supporting gel structure, a process that can be achieved with washing and incubation steps that are mostly familiar to those with experience handling tissue specimens. The greatest drawbacks are its incompatibility with in vivo imaging and the need for continuing validation as researchers apply ExM to the investigation of new subdiffraction limit–sized structures. In part because of the robustness of ExM, numerous groups have begun to independently develop variations on the original method. Such variations include combining it with new contrast agents (e.g., nanoparticles); combining it with existing cutting-edge imaging methods (e.g., light sheet, SIM, STED, and other super-resolution methods); modifying the anchoring step to retain nucleic acids in the gel (e.g., ExFISH); and modifying the fixation, anchoring, gel recipe, and disruption steps to enable improved antibody staining performance after gel embedding (e.g., ultraExM).

At this point, ExM is very well suited for mapping the distribution of nanostructures within thick tissue slices, where precise isotropic preservation of the nanostructure itself is not critical. For the characterization of nanostructures, such as the NPC and other protein complexes, more validation, and indeed more protocol development, is required. The optimized fixation and gel

recipe of ultraExM preserves the structure of isolated centrioles better than the original ExM, but it remains to be seen how well this approach can work in cultured cells and tissue. Further innovation in each step of the process may be useful in achieving isotropic, antigen-preserving expansion across all or most subcellular structures in multiple specimen types, but the robustness and engineerability of ExM make this possibility realistic. Fundamental to super-resolution approaches, markers of organelles and other structures that appear continuous may become punctate when the resolution is beyond the labeling density. Thus, higher-density markers are needed to fully take advantage of the resolution afforded by ExM and its variants.

As ExM democratizes the capability to map and characterize nanostructures, including organelles and protein complexes, both stereotyped and variable, researchers should begin to think about what can be done with this capability in their own fields. Neuroscience offers a particularly compelling case, as the function of a neural circuit is determined by both its connectivity over long distances and the nanoscale structure of synapses. Meanwhile, microbiologists tend to be more comfortable with biochemical methods than imaging, but the diversity of microbes present in different spatial contexts (e.g., microbiomes and biofilms) may present unique opportunities for the application of a simple microscopy method, such as ExM, that can access deep, submicrometer-scale structures (Schlafer & Meyer 2017). As one final example from among many possibilities, the internal structure of the nucleus is currently attracting much attention but is most readily studied in cultured cells (Andrey & Mundlos 2017). Studying these features with subdiffraction-limited resolution over, for example, entire embryos may prove uniquely enabling in terms of connecting the subcellular mechanisms that determine a cell's behavior to the behavior of cells in their normal tissue context.

As more groups independently use and modify the ExM protocol, additional applications will naturally emerge. These should come to play an important role in understanding the nanoscale structure of cells, especially within their tissue context. Perhaps most importantly, ExM allows all labs—not just those with specialized equipment and expertise—to access these structures in their own specimens.

DISCLOSURE STATEMENT

The authors are not aware of any affiliations, memberships, funding, or financial holdings that might be perceived as affecting the objectivity of this review.

ACKNOWLEDGMENTS

F.C. is a Schmidt Fellow funded by Eric and Wendy Schmidt.

LITERATURE CITED

Andrey G, Mundlos S. 2017. The three-dimensional genome: regulating gene expression during pluripotency and development. *Development* 144(20):3646–58

Artur C, Womack T, Eriksen JLJ, Mayerich D, Shih W-C. 2017. Hyperspectral expansion microscopy. In *Proceedings of the 2017 IEEE Photonics Conference*, pp. 23–24. Piscataway, NJ: IEEE

Artur CG, Womack T, Zhao F, Eriksen JL, Mayerich D, Shih W-C. 2018. Plasmonic nanoparticle-based expansion microscopy with surface-enhanced Raman and dark-field spectroscopic imaging. *Biomed. Opt. Express* 9(2):603–15

Beghein E, Gettemans J. 2017. Nanobody technology: a versatile toolkit for microscopic imaging, protein-protein interaction analysis, and protein function exploration. *Front. Immunol.* 8:771–84

Betzig E, Patterson GH, Sougrat R, Lindwasser OW, Olenych S, et al. 2006. Imaging intracellular fluorescent proteins at nanometer resolution. *Science* 313(5793):1642–45

Biederer T, Kaeser PS, Blanpied TA. 2017. Transcellular nanoalignment of synaptic function. *Neuron* 96(3):680–96

Burette AC, Lesperance T, Crum J, Martone M, Volkmann N, et al. 2012. Electron tomographic analysis of synaptic ultrastructure. *J. Comp. Neurol.* 520(12):2697–711

Cahoon CK, Yu Z, Wang Y, Guo F, Unruh JR, et al. 2017. Superresolution expansion microscopy reveals the three-dimensional organization of the *Drosophila* synaptonemal complex. *PNAS* 114(33):E6857–66

Cang H, Tong Z, Beuzer P, Ye Q, Axelrod J, Hong Z. 2016. Ex-STORM: expansion single molecule nanoscopy. bioRxiv 049403. **https://doi.org/10.1101/049403**

Chang J, Chen F, Yoon Y, Jung E, Babcock H, et al. 2017. Iterative expansion microscopy. *Nat. Methods* 14(6):593–99

Chen B-C, Legant WR, Wang K, Shao L, Milkie DE, et al. 2014. Lattice light-sheet microscopy: imaging molecules to embryos at high spatiotemporal resolution. *Science* 346(6208):1257998

Chen F, Tillberg PW, Boyden ES. 2015. Expansion microscopy. *Science* 347(6221):543–48

Chen F, Wassie AT, Cote AJ, Sinha A, Alon S, et al. 2016. Nanoscale imaging of RNA with expansion microscopy. *Nat. Methods* 13(8):679–84

Chhetri RK, Amat F, Wan Y, Höckendorf B, Lemon WC, Keller PJ. 2015. Whole-animal functional and developmental imaging with isotropic spatial resolution. *Nat. Methods* 12(12):1171–78

Chozinski TJ, Halpern AR, Okawa H, Kim H-J, Tremel GJ, et al. 2016. Expansion microscopy with conventional antibodies and fluorescent proteins. *Nat. Methods* 13(April):1–7

Chozinski TJ, Mao C, Halpern AR, Pippin JW, Shankland SJ, et al. 2018. Volumetric, nanoscale optical imaging of mouse and human kidney via expansion microscopy. *Sci. Rep.* 8(1):10396

Chung K, Wallace J, Kim S-Y, Kalyanasundaram S, Andalman AS, et al. 2013. Structural and molecular interrogation of intact biological systems. *Nature* 497(7449):332–37

Costa RP, Mizusaki BEP, Sjöström PJ, van Rossum MCW. 2017. Functional consequences of pre- and postsynaptic expression of synaptic plasticity. *Philos. Trans. R. Soc. B Biol. Sci.* 372(1715):20160153

Crittenden J, Tillberg P, Riad M, Shima Y, Gerfen C, et al. 2016. Striosome-dendron bouquets highlight a unique striatonigral circuit targeting dopamine-containing neurons. *PNAS* 113(40):11318–23

Deshpande T, Li T, Herde MK, Becker A, Vatter H, et al. 2017. Subcellular reorganization and altered phosphorylation of the astrocytic gap junction protein connexin43 in human and experimental temporal lobe epilepsy. *Glia* 65(11):1809–20

Economo MN, Clack NG, Lavis LD, Gerfen CR, Svoboda K, et al. 2016. A platform for brain-wide imaging and reconstruction of individual neurons. *eLife* 5:e10566

Fecher C, Trovò L, Müller SA, Snaidero N, Wettmarshausen J, et al. 2018. Profound functional and molecular diversity of mitochondria revealed by cell type–specific profiling in vivo. bioRxiv 403774. **https://doi.org/10.1101/403774**

Freifeld L, Odstrcil I, Förster D, Ramirez A, Gagnon JA, et al. 2017. Expansion microscopy of zebrafish for neuroscience and developmental biology studies. *PNAS* 114(50):E10799–808

Fulterer A, Andlauer TFM, Ender A, Maglione M, Eyring K, et al. 2018. Active zone scaffold protein ratios tune functional diversity across brain synapses. *Cell Rep.* 23(5):1259–74

Gambarotto D, Zwettler FU, Le Guennec M, Schmidt-Cernohorska M, Fortun D, et al. 2019. Imaging cellular ultrastructures using expansion microscopy (U-ExM). *Nat. Methods* 16(1):71–74

Gao R, Asano SM, Upadhyayula S, Pisarev I, Milkie DE, et al. 2019. Cortical column and whole-brain imaging with molecular contrast and nanoscale resolution. *Science* 363(6424):eaau8302

Germroth PG, Gourdie RG, Thompson RP. 1995. Confocal microscopy of thick sections from acrylamide gel embedded embryos. *Microsc. Res. Tech.* 30(6):513–20

Godin AG, Lounis B, Cognet L. 2014. Super-resolution microscopy approaches for live cell imaging. *Biophys. J.* 107:1777–84

Goonawardane N, Yin C, Harris M. 2018. A pivotal role of serine 225 phosphorylation in the function of hepatitis C virus NS5A revealed with the application of a phosphopeptide antiserum and super-resolution microscopy. bioRxiv 387407. **https://doi.org/10.1101/387407**

Guo F, Holla M, Díaz MM, Rosbash M. 2018. A circadian output circuit controls sleep-wake arousal in *Drosophila*. *Neuron* 100(3):624–35.e4

Guo ZV, Inagaki HK, Daie K, Druckmann S, Gerfen CR, Svoboda K. 2017. Maintenance of persistent activity in a frontal thalamocortical loop. *Nature* 545(7653):181–86

Hafner A-S, Donlin-Asp P, Leitch B, Herzog E, Schuman EM. 2018. Local protein synthesis in axon terminals and dendritic spines differentiates plasticity contexts. bioRxiv 363184. **https://doi.org/10.1101/363184**

Halpern AR, Alas GCM, Chozinski TJ, Paredez AR, Vaughan JC. 2017. Hybrid structured illumination expansion microscopy reveals microbial cytoskeleton organization. *ACS Nano* 11(12):12677–86

Hermanson GT. 2013. *Bioconjugate Techniques*. San Diego, CA: Academic. 3rd ed.

Hörl D, Rusak FR, Preusser F, Tillberg P, Randel N, et al. 2018. BigStitcher: reconstructing high-resolution image datasets of cleared and expanded samples. bioRxiv 343954. **https://doi.org/10.1101/343954**

Huisken J, Stainier DYR. 2009. Selective plane illumination microscopy techniques in developmental biology. *Development* 136(12):1963–75

Ke R, Mignardi M, Pacureanu A, Svedlund J, Botling J, et al. 2013. In situ sequencing for RNA analysis in preserved tissue and cells. *Nat. Methods* 10(9):857–60

Kenney M, Ray S, Boles TC. 1998. Mutation typing using electrophoresis and gel-immobilized acrydite™ probes. *Biotechniques* 25(3):516–21

Kim CK, Yang SJ, Pichamoorthy N, Young NP, Kauvar I, et al. 2016. Simultaneous fast measurement of circuit dynamics at multiple sites across the mammalian brain. *Nat. Methods* 13(4):325–28

Ku T, Swaney J, Park J-Y, Albanese A, Murray E, et al. 2016. Multiplexed and scalable super-resolution imaging of three-dimensional protein localization in size-adjustable tissues. *Nat. Biotechnol.* 34(9):973–81

Kuan L, Li Y, Lau C, Feng D, Bernard A, et al. 2015. Neuroinformatics of the *Allen Mouse Brain Connectivity Atlas. Methods* 73:4–17

Laissue PP, Reiter C, Hiesinger PR, Halter S, Fischbach KF, Stocker RF. 1999. Three-dimensional reconstruction of the antennal lobe in *Drosophila melanogaster*. *J. Comp. Neurol*. 405(4):543–52

Lee JH, Daugharthy ER, Scheiman J, Kalhor R, Yang JL, et al. 2014. Highly multiplexed subcellular RNA sequencing in situ. *Science* 343:1360–63

Li R, Chen X, Lin Z, Wang Y, Sun Y. 2018. Expansion enhanced nanoscopy. *Nanoscale* 10(37):17552–56

Liu Z, Tjian R. 2018. Visualizing transcription factor dynamics in living cells. *J. Cell Biol.* 217(4):1181–91

Mapelli L, Solinas S, D'Angelo E. 2014. Integration and regulation of glomerular inhibition in the cerebellar granular layer circuit. *Front. Cell. Neurosci.* 8:55

Migliori B, Datta MS, Dupre C, Apak MC, Asano S, et al. 2018. Light sheet theta microscopy for rapid high-resolution imaging of large biological samples. *BMC Biol*. 16(1):57

Mosca TJ, Luginbuhl DJ, Wang IE, Luo L. 2017. Presynaptic LRP4 promotes synapse number and function of excitatory CNS neurons. *eLife* 6:e27347

Pena JTG, Sohn-Lee C, Rouhanifard SH, Ludwig J, Hafner M, et al. 2009. miRNA in situ hybridization in formaldehyde and EDC-fixed tissues. *Nat. Methods* 6(2):139–41

Perea G, Navarrete M, Araque A. 2009. Tripartite synapses: Astrocytes process and control synaptic information. *Trends Neurosci*. 32(8):421–31

Pesce L, Cozzolino M, Lanzanò L, Diaspro A, Bianchini P. 2018. Enigma at the nanoscale: Can the NPC act as an intrinsic reporter for isotropic expansion microscopy? bioRxiv 449702. **https://doi.org/10.1101/449702**

Rust MJ, Bates M, Zhuang XW. 2006. Sub-diffraction-limit imaging by stochastic optical reconstruction microscopy (STORM). *Nat Methods* 3(10):793–95

Schlafer S, Meyer RL. 2017. Confocal microscopy imaging of the biofilm matrix. *J. Microbiol. Methods* 138:50–59

Shapira M, Zhai RG, Dresbach T, Bresler T, Torres VI, et al. 2003. Unitary assembly of presynaptic active zones from Piccolo-Bassoon transport vesicles. *Neuron* 38(2):237–52

Südhof TC. 2004. The synaptic vesicle cycle. *Annu. Rev. Neurosci.* 27:509–47

Suofu Y, Li W, Jean-Alphonse FG, Jia J, Khattar NK, et al. 2017. Dual role of mitochondria in producing melatonin and driving GPCR signaling to block cytochrome *c* release. *PNAS* 114(38):E7997–8006

Sylwestrak EL, Rajasethupathy P, Wright MA, Jaffe A, Deisseroth K. 2016. Multiplexed intact-tissue transcriptional analysis at cellular resolution. *Cell* 164(4):792–804

Tanaka T, Fillmore D, Sun ST, Nishio I, Swislow G, Shah A. 1980. Phase transitions in ionic gels. *Phys. Rev. Lett.* 45:1636–39

Tillberg PW, Chen F, Piatkevich KD, Zhao Y, Yu C-C, et al. 2016. Protein-retention expansion microscopy of cells and tissues labeled using standard fluorescent proteins and antibodies. *Nat. Biotechnol.* 34(9):987–92

Truckenbrodt S, Maidorn M, Crzan D, Wildhagen H, Kabatas S, Rizzoli SO. 2018. X10 expansion microscopy enables 25-nm resolution on conventional microscopes. *EMBO Rep*. 19(9):e45836

Tsai A, Muthusamy AK, Alves MR, Lavis LD, Singer RH, et al. 2017. Nuclear microenvironments modulate transcription from low-affinity enhancers. *eLife* 6:e28975

Tsanov N, Samacoits A, Chouaib R, Traboulsi A-M, Gostan T, et al. 2016. smiFISH and FISH-quant—a flexible single RNA detection approach with super-resolution capability. *Nucleic Acids Res*. 44(22):e165

Unnersjö-Jess D, Scott L, Sevilla SZ, Patrakka J, Blom H, Brismar H. 2018. Confocal super-resolution imaging of the glomerular filtration barrier enabled by tissue expansion. *Kidney Int*. 93(4):1008–13

Wang G, Moffitt JR, Zhuang X. 2018. Multiplexed imaging of high-density libraries of RNAs with MERFISH and expansion microscopy. *Sci. Rep.* 8(1):4847

Wang IE, Lapan SW, Scimone ML, Clandinin TR, Reddien PW. 2016. Hedgehog signaling regulates gene expression in planarian glia. *eLife* 5:e16996

Wei L, Chen Z, Shi L, Long R, Anzalone AV, et al. 2017. Super-multiplex vibrational imaging. *Nature* 544(7651):465–70

Whelan DR, Bell TDM. 2015. Image artifacts in single molecule localization microscopy: why optimization of sample preparation protocols matters. *Sci. Rep.* 5(1):7924

Yu JY, Kanai MI, Demir E, Jefferis GSXE, Dickson BJ. 2010. Cellular organization of the neural circuit that drives *Drosophila* courtship behavior. *Curr. Biol.* 20(18):1602–14

Zhang L, Bailey JB, Subramanian RH, Groisman A, Tezcan FA. 2018. Hyperexpandable, self-healing macromolecular crystals with integrated polymer networks. *Nature* 557(7703):86–91

Zhang YS, Trujillo–de Santiago G, Alvarez MM, Schiff SJ, Boyden ES, Khademhosseini A. 2017. Expansion mini-microscopy: an enabling alternative in point-of-care diagnostics. *Curr. Opin. Biomed. Eng.* 1:45–53

Zhao Y, Bucur O, Irshad H, Chen F, Weins A, et al. 2017. Nanoscale imaging of clinical specimens using pathology-optimized expansion microscopy. *Nat. Biotechnol.* 35(8):757–64